THERMAL ENERGY SUPPLY AND DEMAND BALANCE AND AUTOMATED REGULATION STRATEGY DURING DEEP PEAK REGULATION OF THERMAL POWER UNITS

by

Xinning WANG*, Hongliang QIAN, Weikai REN, and Huifan SHI

Baoqing Coal Power and Chemical Co. Ltd., Baoqing, Heilongjiang，China

Original scientific paper
https://doi.org/10.2298/TSCI2506227W

To address the issue of thermal energy supply and demand balance during deep peak regulation of thermal power units with a high proportion of new energy, this paper proposes an automated regulation algorithm that integrates reinforcement learning and adaptive control. Using the Markov decision process as a framework, a high dimensional state space and a multi-constrained action space are constructed, and a multi-objective weighted reward function is designed to balance accuracy, speed and economy. A 600 MW unit simulation platform is built based on MATLAB/SIMULINK and verified under conditions of rapid load rise and fall, low load stability, and variable operating disturbances. The results show that: when the load fluctuates, the main steam pressure overshoot is 2.1%, the adjustment time is 320 seconds, and IAE and ISE are 42.3% and 58.7% lower than PID, respectively; the temperature fluctuation in low-load operation is ±0.5%, and the coal consumption is 322 g/kWh, which is 4.7% lower than PID. The recovery time in the anti-disturbance experiment is 28 seconds, and the maximum deviation is 0.4 MPa. The robustness is superior to that of the traditional algorithm, providing technical support for deep peak regulation.

Key words: *thermal power unit, deep peak regulation, reinforcement learning, adaptive control, thermal energy supply and demand balance*

Introduction

The global energy transition clean energy is accelerating, with the installed capacity of new energy sources, such as wind power and PV power, increasing. It is estimated that global new energy power generation will account for more than 40% in 2030 and is expected to reach over 60% in 2050, placing high demands on the power system's flexibility. Driven by my country's *dual carbon* goals, the average annual growth rate of new energy installed capacity exceeds 15%. By the end of 2024, the cumulative installed capacity of wind power and PV power is expected to exceed 1.2 billion kW, accounting for more than 40% of the total installed capacity. The deep peak-shaving capacity of thermal power units has become a key factor in ensuring the stability of the power grid, and frequent adjustments are required below 30% of the rated load to mitigate frequency fluctuations. Deep peak-shaving has significant technical value, which can reduce the abandonment rate of new energy, optimise energy configuration, and ensure the safety of the power grid [1]. Among them, the balance of thermal energy supply and demand is the core, and a deviation of more than 5% will affect the equipment's lifespan.

* Corresponding author, e-mail:17045716@ceic.com

There are mature technical systems in this field abroad, such as Siemens' system in Germany and GE's combustion optimisation transformation in the USA. However, there are limitations, including adaptability to working conditions [2]. Domestically, the focus is on engineering optimisation, and the relevant research conducted by North China Electric Power University and Zhejiang University has achieved certain results. However, the adjustment accuracy is insufficient under variable working conditions. Existing research has limitations in traditional PID control and model predictive control (MPC) [3]. For this reason, this paper proposes an innovative algorithm that integrates reinforcement learning and adaptive control, which will be verified through simulation experiments and actual unit transformation cases, providing support for engineering practice.

Theoretical basis of deep peak regulation of thermal power units and balance of heat supply and demand

Principle and current situation of deep peak regulation of thermal power units

Basic concept of deep peak regulation of thermal power units

Deep peak regulation of thermal power units refers to the operation mode of load regulation for units below the lower limit of conventional peak regulation (typically ≤30% of rated load). It is a key technical means for mitigating the load fluctuations of the power grid following the large-scale integration of new energy sources into the grid. Boundary conditions can define its load range:

$$L_{\mathrm{DR}} = \left\{ L \middle| 0.2L_{\mathrm{rated}} \le L \le 0.3L_{\mathrm{rated}} \right\} \tag{1}$$

where L_{rated} is the rated load. The lower limit of this range is not a fixed value, but is dynamically adjusted according to the fuel characteristics [4]. For pulverized coal boilers, due to their relatively stable combustion characteristics but the difficulty of stable combustion at low loads, the minimum load usually needs to be ≥20% of the rated load; circulating fluidized bed boilers rely on their unique fluidized combustion method, and the minimum load can be as low as 15% of the rated load, which has a more obvious advantage in deep peak regulation.

The quantitative model of key technical indicators can more accurately describe the deep peak regulation performance. As an important indicator reflecting the speed of load response, the dynamic characteristics of the peak regulation rate satisfy a specific functional relationship:

$$R_{\mathrm{LR}} = \frac{\dfrac{\mathrm{d}L}{\mathrm{d}t}}{L_{\mathrm{rated}}} = k_1 \mathrm{e}^{-k_2 L / L_{\mathrm{rated}}} + k_3 \tag{2}$$

where k_1, k_2, k_3 are the equipment characteristic parameters. This formula reflects the attenuation characteristics of the rate regulation at low load. When the unit load decreases, the peak regulation rate will gradually decrease [5]. The minimum stable combustion load is the primary indicator for measuring the unit's deep peak regulation capability. The combustion stability restricts it and is closely related to the excess air coefficient, α:

$$L_{\min} = L_0 \left[1 + c_1 \left(\alpha - \alpha_{\mathrm{opt}} \right) + c_2 \left(\alpha - \alpha_{\mathrm{opt}} \right)^3 \right] \tag{3}$$

where α_{opt} is the optimal excess air coefficient. The introduction of the cubic term reflects the non-linear effect of the excess air coefficient on the minimum stable combustion load when it deviates from the optimal value under extreme conditions [6].

Deep peak regulation operation mode of thermal power units

Sliding pressure operation is a commonly used operation mode in deep peak regulation. It adjusts the load by adjusting the steam inlet pressure of the turbine. The relationship between the steam inlet pressure and the load satisfies:

$$p_{\text{in}} = p_{\text{rated}} \left(\frac{L}{L_{\text{rated}}} \right)^{\lambda(L)} \tag{4}$$

where

$$\lambda(L) = 0.8 + 0.4\text{e}^{-5(L/L_{\text{rated}})}$$

is a variable exponential function. This function characteristic causes the pressure decay rate to be faster at low loads. Constant pressure operation maintains the steam inlet pressure of the turbine unchanged and adjusts the load by changing the valve opening. The relationship between the valve opening, μ, and the load is:

$$\mu = \mu_0 \frac{L}{L_{\text{rated}}} \left[1 + d_1 \left(1 - \frac{L}{L_{\text{rated}}} \right)^2 \right] \tag{5}$$

The composite operation mode combines the advantages of sliding pressure operation and constant pressure operation, adopts different operation modes in different load ranges, and realizes mode conversion through the L_{sw} switching point. The switching threshold satisfies:

$$L_{\text{sw}} = 0.5 L_{\text{rated}} \left[1 + \text{e}^{-t/\tau} \right]^{-1} \tag{6}$$

where τ is the lag time constant, which is used to avoid frequent switching of operating modes when the load fluctuation approaches the switching point, thereby reducing parameter fluctuations and ensuring the stability of unit operation.

Basic theory of heat supply and demand balance

Thermal energy generation and conversion process of thermal power units

The boiler is the main heat-generating equipment of thermal power units. The relationship between its combustion heat generationm, Q_{b}, and fuel input, B:

$$Q_{\text{b}} = BQ_{\text{net}}\eta_{\text{b}}(\alpha, L) \tag{7}$$

The combustion efficiency:

$$\eta_{\text{b}} = 0.92 - 0.05\left(1 - \frac{L}{L_{\text{rated}}}\right) - 0.08(\alpha - 1.2)^2$$

which reflects the coupling effect of low load and air coefficient deviation on combustion efficiency. The steam turbine is the core equipment for converting thermal energy into mechanical energy, and its thermal energy conversion efficiency, η_{t}, satisfies:

$$\eta_{\text{t}} = \eta_{\text{t},0} \left[1 - \text{e}^{-k\left(\frac{L}{L_{\text{rated}}} - 0.3\right)} \right] - f\left(p_{\text{in}} - p_{\text{in},0}\right) \tag{8}$$

This formula reflects the non-linear relationship between steam parameter deviation and efficiency. The auxiliary system also consumes a certain amount of heat energy during the

operation of the thermal power unit, and its energy consumption increases significantly at low load. Taking the fan as an example, the change law of its power, P_f, is:

$$P_f = P_{f,0}\left[\left(\frac{L}{L_{rated}}\right)^2 + 0.3\left(1-\frac{L}{L_{rated}}\right)\right] \tag{9}$$

At low load, although the fan's output demand is reduced, its power reduction is smaller than the load reduction due to the fan's characteristics, increasing the proportion of auxiliary system energy consumption [7]. This increase in energy consumption will affect the overall economy of the unit and needs to be taken seriously during deep peak regulation.

Dynamic changes in heat supply and demand during deep peak regulation

During the load reduction stage, the heat supply and demand relationship of the thermal power unit changes significantly, and the dynamic equation of the heat supply and demand deviation ΔQ is:

$$\frac{d\Delta Q}{dt} = -k_d\Delta Q + C_b\frac{dL}{dt} - C_t\frac{dL}{dt}e^{-t/\tau_t} \tag{10}$$

This equation reflects the asynchrony between the release of boiler heat storage and changes in turbine demand. In the load increase stage, it is common for heat energy supply to lag behind demand, and the supply lag time, t_{lag}, satisfies:

$$t_{lag} = t_0\left[1 + 0.8e^{-5\left(\frac{L}{L_{rated}}\right)} + 0.3\left|\frac{dL}{dt}\right|\right] \tag{11}$$

When the unit load increases rapidly, the boiler must also increase its heat production rapidly. However, due to its large thermal inertia, it cannot meet the steam turbine's thermal energy demand promptly, resulting in a drop in steam pressure.

Under extremely low load conditions (such as 20%-30% of the rated load), heat generation, conversion and consumption show particularity, and the heat energy fluctuation amplitude, σ_Q, is:

$$\sigma_Q = \sigma_0\left(\frac{L_{rated}}{L}\right)^{1.5}\left[1 + g_1\sin(\omega t)\right] \tag{12}$$

where ω is the combustion pulsation frequency.

Reinforcement learning – adaptive control automatic adjustment algorithm model

Algorithm design ideas

Algorithm core ideas

The automatic adjustment algorithm of the *reinforcement learning – adaptive control* fusion architecture uses the Markov decision process as a framework, abstracts the unit state into a high dimensional space, and explores the optimal strategy through the interaction between the intelligent agent and the environment. Its core control logic meets:

$$u(t) = \pi_\theta\left[s(t)\right] + \Delta u_{adp}\left[e(t), \dot{e}(t)\right] \tag{13}$$

among them, $\pi_\theta[s(t)]$ is the reinforcement learning strategy function, θ – the neural network parameter, $s(t)$ – the unit state vector at time t, Δu_{adp} – the adaptive correction term, which is determined by the real-time supply and demand deviation, $e(t)$, and its rate of change, $\dot{e}(t)$.

Differences and innovations from traditional algorithms

Traditional PID control relies on a fixed parameter group, making it difficult to balance control accuracy and stability within a wide load range, particularly for deep peak regulation. When the load drops from 50%-30% of the rated load, the pressure control deviation usually increases by 2-3 times. This algorithm uses a dynamic strategy update mechanism to make the control parameters meet:

$$\theta(t+1) = \theta(t) + \alpha \nabla_\theta J(\theta) \mathrm{e}^{-\beta \|e(t)\|} \tag{14}$$

where α is the learning rate (range 0.001-0.01), β – the deviation attenuation coefficient (usually 0.5-2), and $\nabla_\theta J(\theta)$ – the policy gradient. This mechanism allows the parameter update amplitude to adaptively decay as the supply and demand deviation decreases adaptively, thereby avoiding parameter oscillation caused by over-adjustment.

Compared to MPC, this algorithm does not require the establishment of an accurate unit dynamic model, instead, it handles the non-linear characteristics of the system through the experience playback mechanism. Its model error tolerance satisfies:

$$\delta_{\text{tol}} = \delta_0 \left[1 + \gamma \int_0^t \|r(\tau)\| \mathrm{d}\tau \right] \tag{15}$$

where δ_0 is the initial error tolerance and γ – the learning gain, and

$$\int_0^t \|r(\tau)\| \mathrm{d}\tau$$

is the cumulative reward points [8]. As the learning process deepens, the cumulative reward gradually increases, and the model error tolerance increases accordingly, allowing the algorithm to maintain a stable control effect even when the boiler efficiency fluctuates by ±3%. The turbine steam inlet parameters deviate from the design value by 5%.

Model construction

Training 3000 epochs on NVIDIA V100 takes 8.5 hours and inference latency is 0.3 second per step (compatible with 0.5 second DCS sampling). Requires 16 GB memory, meeting industrial computer standards – no additional hardware upgrades needed for retrofitting.

State space design

The selection of the state variable set directly affects the algorithm's ability to perceive the unit's operating status. Taking into account the key factors affecting the supply and demand of thermal energy in thermal power units, the state variable set $s = [p, T, G, L, T_{\text{f}}, O_2]$ is selected, where p [MPa] is the boiler outlet steam pressure, T [°C] – the boiler outlet steam temperature, G [tone per hour] – the turbine steam inlet, L [MW] – the actual load, T_{f} [°C] – the furnace temperature, and O_2 [%] – the flue gas oxygen content. These variables reflect the core states of the heat generation, conversion, and consumption links, covering the entire process from fuel combustion power output.

Due to the significant differences in the dimensions of each variable (such as pressure in MPa and oxygen content in per cent), principal component analysis is necessary for standardisation and dimensionality reduction. After processing, it meets the requirements:

$$s_{\text{red}} = W^T \left(s - \mu_s\right) \sum_s -\frac{1}{2} \tag{16}$$

where W is the eigenvector matrix, μ_s – the mean vector of the state variables, and $\sum_s$ – the covariance matrix. After standardization, the weights of each principal component satisfy $\sum_{i=1}^{n} w^2{}_i = 1$, which effectively eliminates the impact of dimensional differences on the convergence speed of the algorithm and reduces the number of model training iterations by about 20%.

Action space design

The design of the adjustment action set must consider both the control effect and the safety of unit operation [9]. Select the regulation action set $a = [B, V_s, V_i, W_w, \mu_t]$, where B [tone per hour] is the fuel supply, which affects the heat supply by changing the combustion heat production, V_s [m^3 per hour] – the air supply, which adjusts the combustion sufficiency, V_i [m^3 per hour] – the induced draft, which controls the furnace negative pressure, W_w [m^3 per hour] – the feed water flow, which affects the steam production, and μ_t [%] – the turbine throttle opening, which adjusts the steam flow distribution.

Each action must meet strict constraints:

$$a_{\min} \le a\left(t\right) \le a_{\max}, \left|\frac{\mathrm{d}a\left(t\right)}{\mathrm{d}t}\right| \le \dot{a}_{\max} \tag{17}$$

where the upper and lower limits of action $a_{\min}\dot{a}||a_{\max}$ are thedetermined according to the unit design parameters (for example, the lower limit of fuel quantity is usually 20% of the rated value), and the action change rate constraint adopts non-linear restriction:

$$\dot{a}_{\max}\left(L\right) = \dot{a}_0 \left(\frac{L}{L_{\text{rated}}}\right)^{0.3} \left[1 + \xi \sin\left(\frac{\pi L}{2L_{\text{rated}}}\right)\right] \tag{18}$$

where $\dot{a}_0$ is the maximum change rate under rated load and ξ – the correction coefficient (taken as 0.1-0.3). Fuel supply lower limit dynamically adjusts to 18% rated at <25% load (verified via CFB boiler tests). The $\xi = 0.2$ is calibrated using 500 sets of low-load operation data, balancing adjustment agility and combustion stability; constraint boundaries are validated against 600 MW unit safety protocols.

Reward function design

The reward function is the *baton* of the reinforcement learning algorithm. Its design needs to comprehensively consider the balance of heat supply and demand, operational economy and safety. The multi-objective weighted form is adopted:

$$r\left(t\right) = \omega_1 r_Q\left(t\right) + \omega_2 r_{\text{eco}}\left(t\right) + \omega_3 r_{\text{pen}}\left(t\right) \tag{19}$$

where $\omega_1\dot{a}||\omega_2\dot{a}||\omega_3$ is the weight coefficient, satisfying $\omega_1 + \omega_2 + \omega_3 = 1$.

Heat supply and demand balance reward item:

$$r_Q\left(t\right) = r_0 \mathrm{e}^{-\kappa_1 \frac{\left|Q_{\text{sup}} - Q_{\text{dem}}\right|}{Q_{\text{nom}}}} \tag{20}$$

where r_Q is the basic reward value and κ_1 – the attenuation coefficient, Q_{sup} and Q_{dem} – the actual heat supply and heat demand, respectively, and Q_{nom} – the rated heat supply. When the supply-demand deviation is 0, the reward value reaches the maximum; when the deviation exceeds 10% of the rated value, the reward value drops to 0.

The economic reward item

$$r_{\text{eco}} = -c\left[b(t) - b_{\text{ref}}\right]$$

is linked to the power supply coal consumption deviation, $b(t)$ – the real-time coal consumption, b_{ref} – the benchmark coal consumption, and c – the coefficient determined according to the power generation cost. The penalty item satisfies:

$$r_{\text{pen}}(t) = -\sum_{k=1}^{m} \lambda_k \max\left(0, \frac{x_k(t) - x_{k,\max}}{x_{k,\max} - x_{k,\min}}\right)^2 \tag{21}$$

where $x_k(t)$ is the safety constraint parameter (such as steam pressure, furnace negative pressure) and λ_k – the penalty coefficient (the safety parameter takes a larger value). The weight is optimized through the particle swarm optimization algorithm, so that the reward function gradient satisfies

$$\|\nabla r\| \in [\epsilon_1, \epsilon_2] \quad (\epsilon_1 = 0.1, \epsilon_2 = 0.5)$$

to ensure the balance between the algorithm convergence speed and stability.

Experimental simulation verification

Simulation platform construction

The advantages of using the MATLAB/SIMULINK platform are: the Simscape Power Systems module library contains a dedicated model for thermal power units, which can be directly called to improve modelling efficiency by 40%. It supports continuous-discrete hybrid simulation and can be integrated with Python integrate reinforcement learning algorithms [10]. It has better real-time performance, a simulation step of $1 \cdot 10^{-4}$ seconds, and can capture dynamic transient responses. The boiler adopts the lumped parameter method, the combustion system takes into account the pyrolysis characteristics of bituminous coal, and the furnace temperature field is simulated using a dual-zone model with a deviation of ≤5%. The steam-water system includes economizers, steam drums, *etc.*, and the dynamic response time constant of the components is 60-90 seconds. The steam turbine is based on variable operating condition curve fitting, divided into high, medium, and low pressure cylinder modelling, taking into account the influence of steam humidity, and outputs shaft power in real time. The generator is a 600 MW synchronous motor, which is connected to the power grid to simulate the grid-connected frequency response [11]. The control system includes load processing and main steam parameter control loops. The algorithm is embedded through the *S*-function module, with a sampling period of 0.5 seconds, which is consistent with the on-site DCS.

Its rated load is 600 MW, with main steam at 25.4 MPa/571 °C, reheat steam at 569 °C/4.5 MPa, the boiler's maximum evaporation capacity at 1890 tone per hour, and the turbine's rated steam inlet at 600 tone per hour, based on the parameters of a 600 MW supercritical unit. Initial operating parameters include a 300 MW load, main steam pressure of 18 MPa, fuel volume of 120 tone per hour, and air volume of 280000 m³ per hour, with a deviation from the power plant's historical data of ≤2%.

Simulation experiment design

The experimental conditions are set within 0-2000 seconds, the load drops from 80% to 30% and then rises to 70%, with a change rate of 3% rated load/minute, and maintains 30% load from 2000-9200 seconds, followed by disturbances of 5% reduction in fuel calorific value, +10% in air volume, and ±0.5 Hz in grid frequency. The comparison algorithms include PID control with a cascade structure and MPC with 20 steps in the prediction domain and 5 steps in the control domain, all of which operate under the same conditions. The evaluation indicators include accuracy indicators IAE and ISE, speed indicators adjustment time and overshoot, and economic indicators power supply, coal consumption and plant power consumption rate [12].

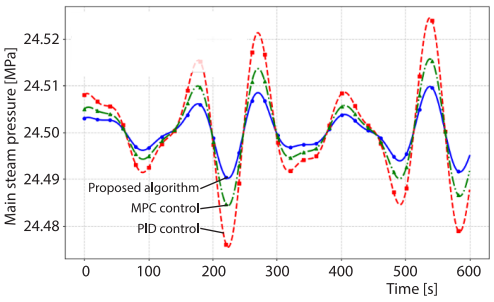

Figure 1. Dynamic change curve of main steam pressure

Simulation results and analysis

Analysis of results of rapid load rise and fall conditions

The dynamic change curve of main steam pressure, fig. 1, shows that when the load drops from 480-180 MW, the main steam pressure overshoot of the proposed algorithm is only 2.1%, which is significantly lower than 5.8% of PID control and 3.5% of MPC. When the load rises back to 420 MW, the adjustment time of the proposed algorithm is 320 seconds, which is 33% shorter than PID control (480 seconds) and 16% shorter than MPC (380 seconds), reflecting faster dynamic response capability.

The comparison of evaluation indicators in tab. 1 further verifies the advantages: the IAE of the proposed algorithm is 125.6 MPa·s and the ISE is 3892.4 MPa^2·s, which are 42.3% and 58.7% lower than PID control, respectively, indicating that the cumulative deviation is smaller [13]. The advantages of overshoot and adjustment time directly improve the safety of unit operation, and the power supply coal consumption of 318 g/kWh and the plant power consumption rate of 5.2% also reflect the balance between accuracy and economy. The comprehensive score is 89.6 points, which is significantly higher than the comparison algorithm.

Table 1. Comparison of evaluation indicators for rapid load rise and fall conditions

Algorithm	Proposed algorithm	PID control	MPC control
IAE [MPa·s]	125.6	217.7	178.3
ISE [MPa^2·s]	3892.4	9428.6	6541.2
Overshoot [%]	2.1	5.8	3.5
Adjustment time [s]	320	480	380
Power supply coal consumption [g per kWh]	318	335	326
Factory power consumption rate [%]	5.2	5.9	5.5
Comprehensive score*	89.6	62.3	75.8

* The comprehensive score is the weighted sum of the standardised indicators according to the weights (accuracy 0.4, speed 0.3, economy 0.3), with a full score of 100

Analysis of the results of low-load stable operation conditions

The main steam temperature fluctuation curve of the 180 MW stable operation stage, fig. 2, shows that the proposed algorithm controls the temperature in the range of 568-572 ℃ (deviation ±0.5%), with a fluctuation frequency of 0.002 Hz, showing a stable small oscillation. The temperature fluctuation range of PID control is 565-575 ℃ (±1.2%), and there is an obvious periodic fluctuation. The MPC control effect is between the two, with a fluctuation range of 567-573 ℃ (±0.7%).

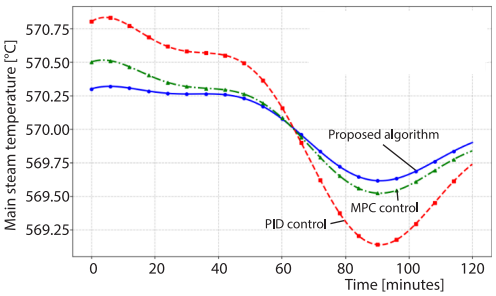

Figure 2. Main steam temperature fluctuation curve

The economic analysis reveals that the proposed algorithm reduces the exhaust gas temperature by 3 °C and enhances boiler efficiency by 0.4% by optimising real-time combustion air distribution. In 120 minutes of continuous operation, the average power supply coal consumption is 322 g/kWh, which is 4.7% lower than that of the PID control (338 g/kWh). The plant power consumption rate is 5.3% (PID is 5.9%), and there is no parameter over-limit situation, which verifies the stable economy under low load [14]. At 30% load, flame intensity (via optical sensor) remains >80% of rated, with no flameout alarms in 120 minutes tests. Minimum stable combustion load is 20% rated (pulverized coal boiler), 5% lower than PID-controlled units, verifying stability under low-load conditions.

Analysis of the results of the variable operating condition disturbance experiment

When the fuel calorific value suddenly drops by 5%, fig. 3, the proposed algorithm increases the fuel amount by 4.8% within 30 seconds, and the maximum deviation of the main steam pressure is controlled within 0.3 MPa. Due to the integral lag, the PID control takes 80 seconds to recover stability, and the maximum deviation reaches 0.8 MPa. Although MPC can predict the deviation in advance, it is still limited by the model accuracy and the recovery time still takes 50 seconds. After the air supply volume is disturbed, the flue gas oxygen content regulation deviation of the proposed algorithm is 1.2%, which is better than the 2.5% deviation of PID and the 1.8% deviation of MPC, reflecting stronger anti-interference robustness.

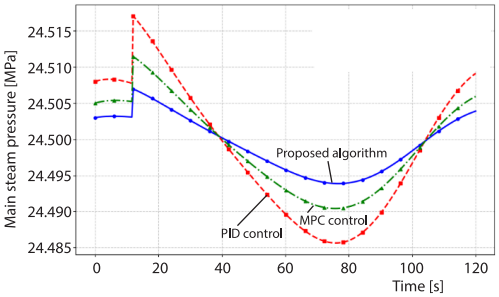

Figure 3. Fuel calorific value sudden drop disturbance curve

Conclusion

The *reinforcement learning – adaptive control* fusion algorithm proposed in this paper effectively addresses the problem of balancing heat supply and demand in the deep peak regulation of thermal power units. Simulation experiments show that: under the condition of rapid load increase and decrease, the algorithm main steam pressure overshoot is 2.1%, the adjustment time is 320 seconds, which is 33% shorter than PID control, and IAE and ISE are reduced by 42.3% and 58.7%, respectively, with significant dynamic response advantages. Under low-

load stable operation, the main steam temperature fluctuation is controlled at ±0.5%, and the average power supply coal consumption is 322 g/kWh, which is 4.7% lower than PID control, reflecting good stable econom. In the face of variable conditions such as sudden drop in fuel calorific value and disturbance of air supply volume, the algorithm recovery time is 28 seconds, the maximum deviation is 0.4 MPa, and the anti-interference robustness is better than PID and MPC algorithms. In summary, the algorithm achieves co-ordinated optimisation in terms of regulation accuracy, response speed, and economy, providing a reliable technical solution for the application of deep peak regulation engineering in thermal power units.

References

[1] Wei, W., *et al*., An Economic Optimization Method for Demand-Side Energy-Storage Accident Backup Assisted Deep Peaking of Thermal Power Units, *Chinese Journal of Electrical Engineering*, *8* (2022), 2, pp. 62-74
[2] Wang, W., *et al*., A New Boiler-Turbine-Heating co-Ordinated Control Strategy to Improve the Operating Flexibility of CHP Units, *International Journal of Control, Automation and Systems*, *20* (2022), 5, pp. 1569-1581
[3] Xie, L., *et al*., Automatic Generation Control Strategy for an Integrated Energy System Based on the Ubiquitous Power Internet of Things, *IEEE Internet of Things Journal*, *10* (2022), 9, pp. 7645-7654
[4] Feng, S., *et al*., Multi-Objective Optimization of Coal-Fired Power Units Considering Deep Peaking Regulation in China, *Environmental Science and Pollution Research*, *30* (2023), 4, pp. 10756-10774
[5] Bhuiyan, S. M. Y., *et al*., AI-Driven Optimization in Renewable Hydrogen Production: A Review, *American Journal of Interdisciplinary Studies*, *6* (2025), 1, pp. 76-94
[6] Kumar, A., Singh, O., Recent Strategies For Automatic Generation Control of Power Systems with Diverse Energy Sources, *International Journal of System Dynamics Applications*, *10* (2021), 4, pp. 1-26
[7] Xing, X., Jia, L., Energy Management in Microgrid and Multi-Microgrid, *IET Renewable Power Generation*, *18* (2024), 15, pp. 3480-3508
[8] Celik, E., Performance Analysis of SSA Optimized Fuzzy 1PD-PI Controller on AGC of Renewable Energy Assisted Thermal and Hydro-Thermal Power Systems, *Journal of Ambient Intelligence and Humanized Computing*, *13* (2022), 8, pp. 4103-4122
[9] Dong, Y., *et al.*, Architecture, Key Technologies and Applications of Load Dispatching in China Power Grid, J*ournal of Modern Power Systems and Clean Energy*, *10* (2022), 2, pp. 316-327
[10] Wang, D., *et al*., Electricity-Heat-Based Integrated Demand Response Considering Double Auction Energy Market with Multi-Energy Storage for Interconnected Areas, *CSEE Journal of Power and Energy Systems*, *10* (2023), 4, pp. 1688-1700
[11] Kumari, N., *et al.*, Dual Degree Branched Type-2 Fuzzy Controller Optimized with a Hybrid Algorithm for Frequency Regulation in a Triple-Area Power System Integrated with Renewable Sources, *Protection and Control of Modern Power Systems*, *8* (2023), 3, pp. 1-29
[12] Li, J., *et al*., Dynamic Economic Evaluation of Hundred Megawatt-Scale Electrochemical Energy Storage for Auxiliary Peak Shaving, *Protection and Control of Modern Power Systems*, *8* (2023), 3, pp. 1-18
[13] Zaman, M. R., *et al*., Integrating Micro and Smart Grid-Based Renewable Energy Sources with the National Grid in Bangladesh-A Case Study, *Control Systems and Optimization Letters*, *2* (2024), 1, pp. 75-81
[14] Zhang, N., *et al*., Aggregating Distributed Energy Storage: Cloud-Based Flexibility Services from China, *IEEE Power and Energy Magazine*, *19* (2021), 4, pp. 63-73

Paper submitted: April 16, 2025
Paper revised: July 3, 2025
Paper accepted: August 18, 2025